Electronic Supplementary Material (ESI) for Inorganic Chemistry Frontiers.

Electronic Supplementary Information

Constructing oxygen-doped g-C_3N_4 nanosheet with enlarged conductive band edge for enhanced visible-light-driven hydrogen evolution

Shaodong Sun,[*a] Jia Li,[a] Jie Cui,[a] Xufeng Gou,[a] Qing Yang,[a] Shuhua Liang,[*a] Zhimao Yang,[b] and Jianmin Zhang[c]

[a] *Shaanxi Province Key Laboratory for Electrical Materials and Infiltration Technology, School of Materials Science and Engineering, Xi'an University of Technology, Xi'an 710048, ShaanXi, People's Republic of China.*

[b] *School of Science, State Key Laboratory for Mechanical Behavior of Materials, MOE Key Laboratory for Non-Equilibrium Synthesis and Modulation of Condensed Matter, Center of Suzhou Nano Science and Technology, Xi'an Jiaotong University, Xi'an 710049, ShaanXi, People's Republic of China.*

[c] *College of Physics and Information Technology, Shaanxi Normal University, Xi'an 710062, ShaanXi, People's Republic of China.*

**Corresponding author.*

E-mail: sdsun@mail.xjtu.edu.cn, liangsh@xaut.edu.cn

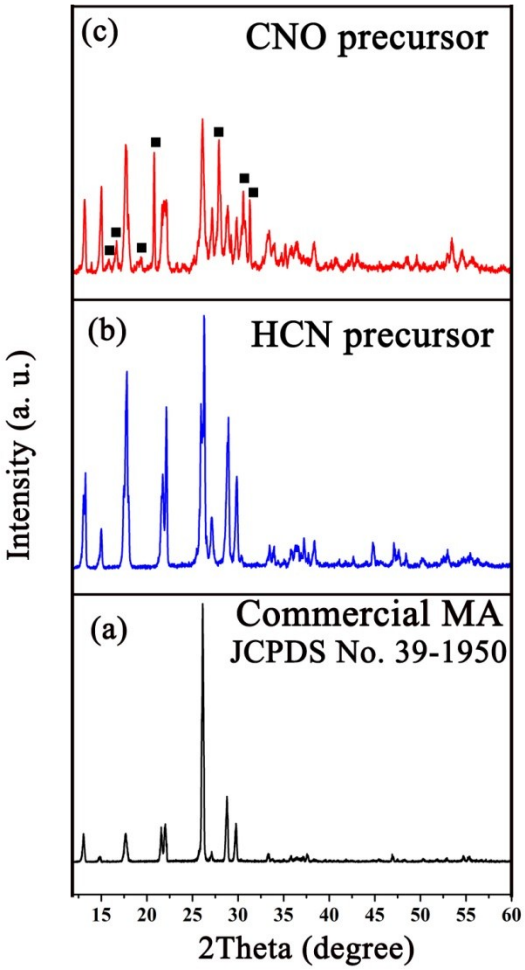

Fig. S1 XRD patterns of the different precursors. (a) Commercial MA (denoted as CN sample); (b) Precursor of the hydrothermally treated MA in the absence of H_2O_2 (denoted as HCN sample) (c) Precursor of the hydrothermally treated MA in the presence of H_2O_2 (denoted as CNO sample).

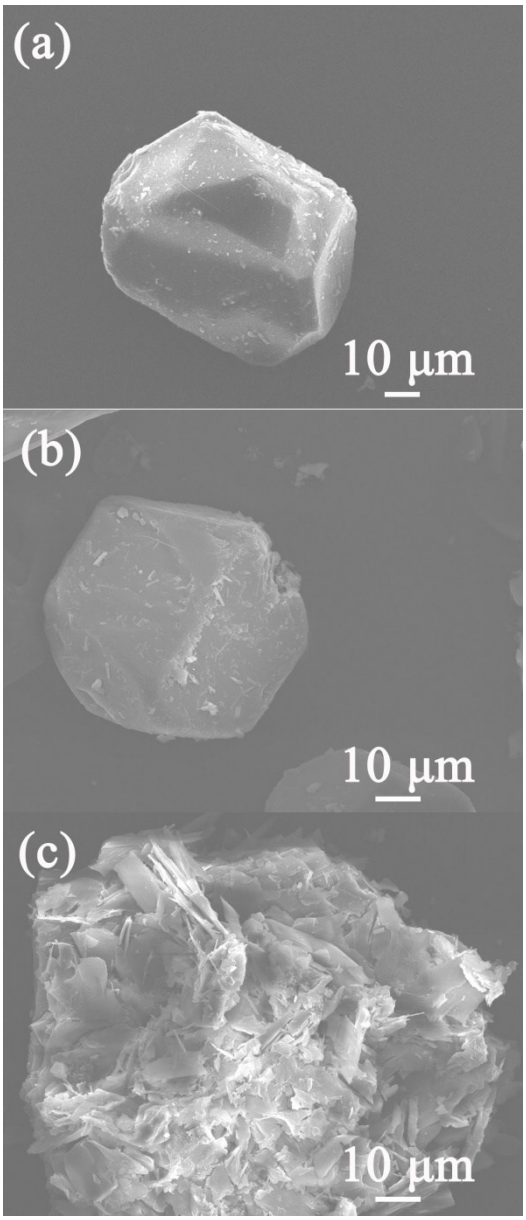

Fig. S2 SEM images of the different precursors. (a) Precursor of CN sample; (b) Precursor of HCN sample (c) Precursor of CNO sample.

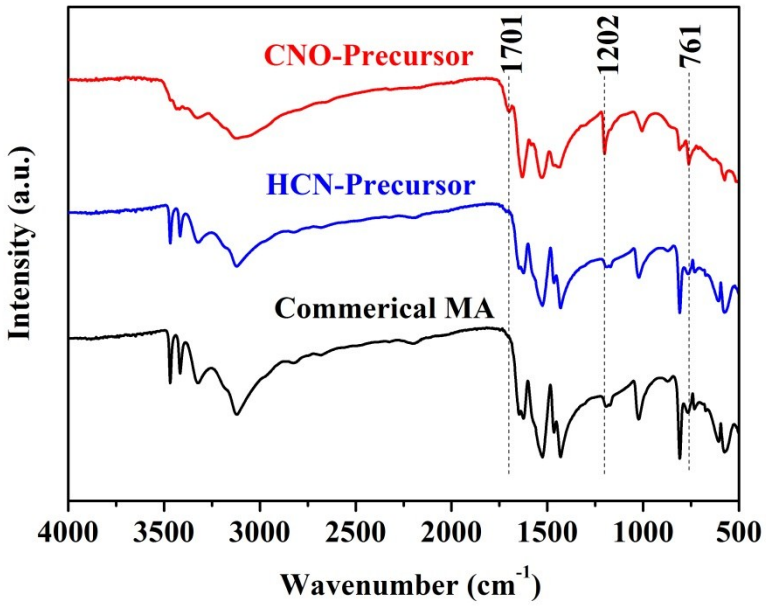

Fig. S3 FTIR spectra of the different precursors. (a) Precursor of CN sample; (b) Precursor of HCN sample (c) Precursor of CNO sample.

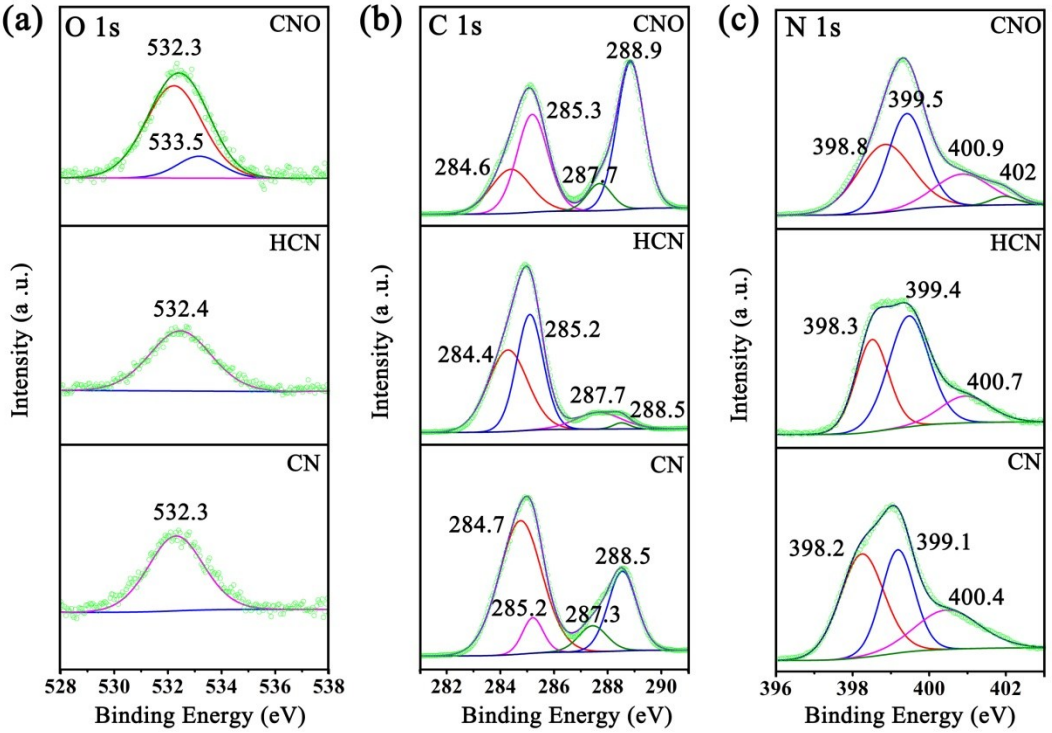

Fig. S4 XPS data of the CN, HCN and CNO sample. (a) High-resolution O 1s spectra; (b) High-resolution C 1s spectra; (c) High-resolution N 1s spectra.

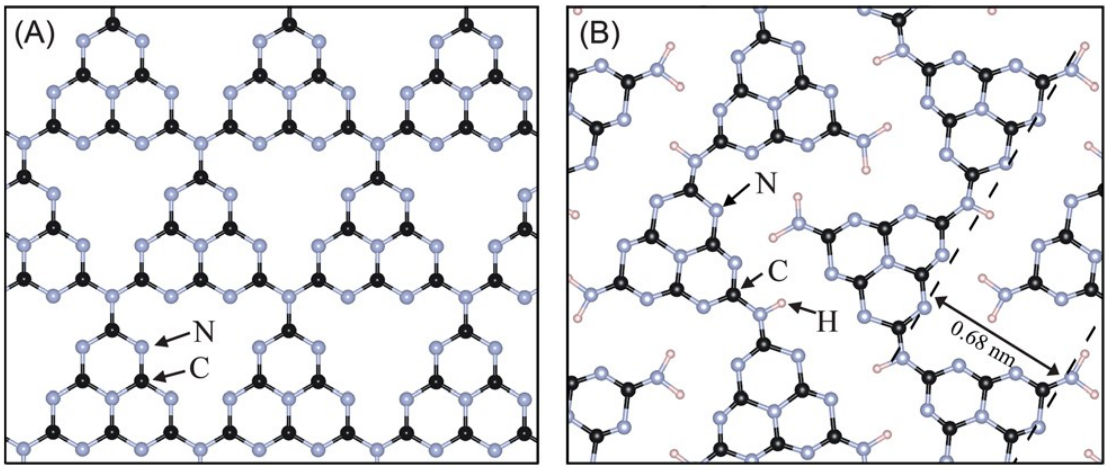

Fig. S5 Structure models of carbon-nitride sheets of (A) perfect g-C_3N_4 and (B) polymeric melon proposed by Lotsch et al.

Fig. S5 displays two models of carbon-nitride sheet structures. It can be found that model A is the sheet structure of "perfect g-C_3N_4" where each tri-s-triazine unit is connected to three tri-s-triazine units with bridging nitrogen atoms (ternary amine). Model B is the sheet structure proposed by Lotsch et al. [*B. V. Lotsch, M. Doblinger, J. Sehnert, L. Seyfarth, J. Senker, O. Oeckler and W. Schnick, Chem.–Eur. J., 2007, 13, 4969–4980.*] A primary amino group (–NH_2) and a secondary amino group (–NH–) are contained in this model. The carbon nitride sheet is composed of one-dimensional chains of NH-bridged tri-s-triazine units, which adopt a "zigzag-type" geometry to reduce the repulsion between the neighboring tri-s-triazine units, and are tightly linked by hydrogen bonds to form a 2-dimensional planar array. [*T. Sano, S. Tsutsui, K. Koike, T. Hirakawa, Y. Teramoto, N. Negishi and K. Takeuchi, J. Mater. Chem. A, 2013,* ***1****, 6489–6496.*]

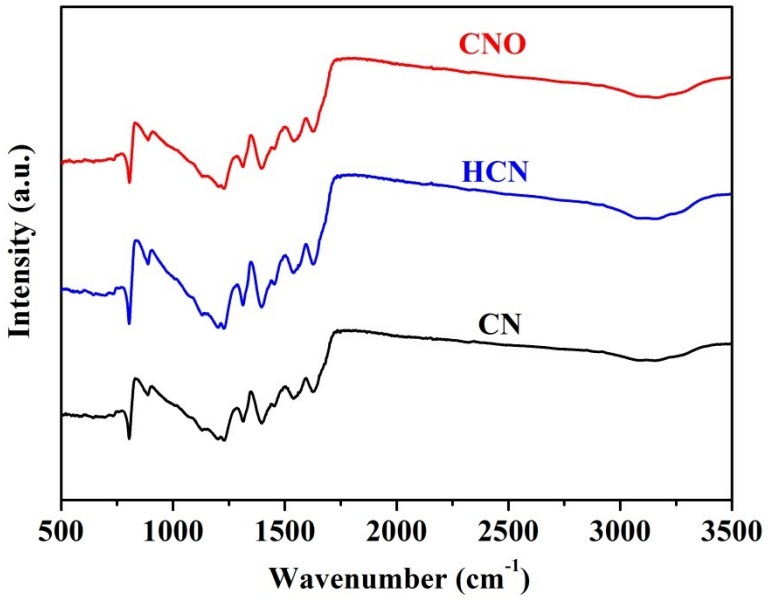

Fig. S6 FTIR spectra of the as-synthesized g-C_3N_4 products. (a) CN sample; (b) HCN sample (c) CNO sample.

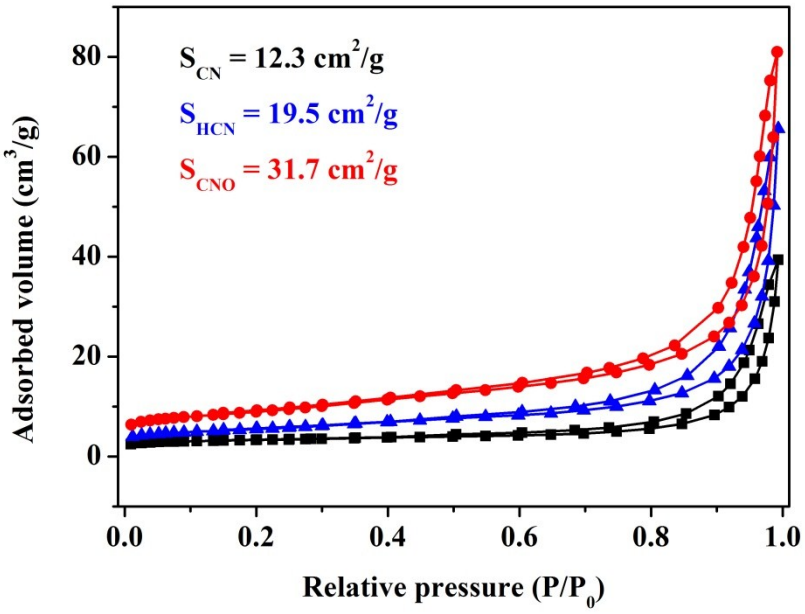

Fig. S7 Nitrogen adsorption-desorption isotherms and specific surface area (the insert) of the as-synthesized CN, HCN and CNO samples.

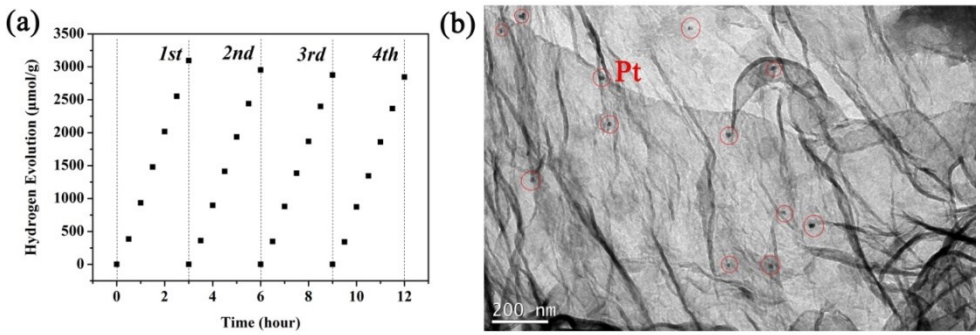

Fig. S8 (a) Recycling of CNO sample for photocatalytic hydrogen evolution. (b) TEM image of the CNO sample for photocatalytic hydrogen production after the fourth cycle.

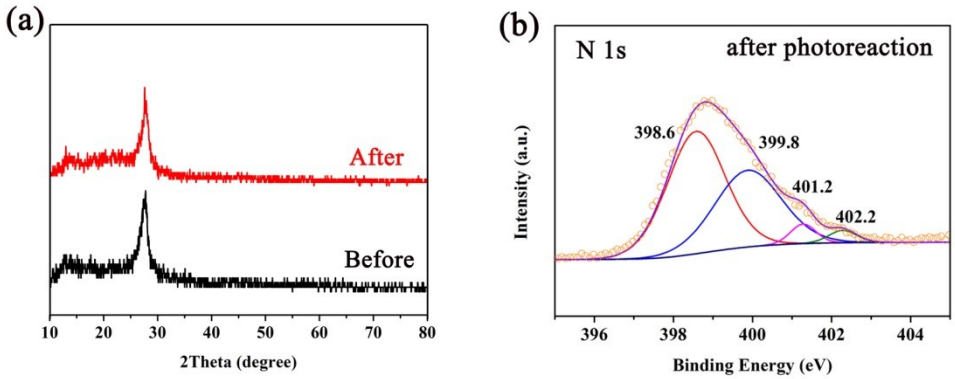

Fig. S9 (a) XRD patterns of the CNO sample for photocatalytic hydrogen production before and after the fourth cycle. (b) N 1s XPS spectrum of the CNO sample for photocatalytic hydrogen production after the fourth cycle.

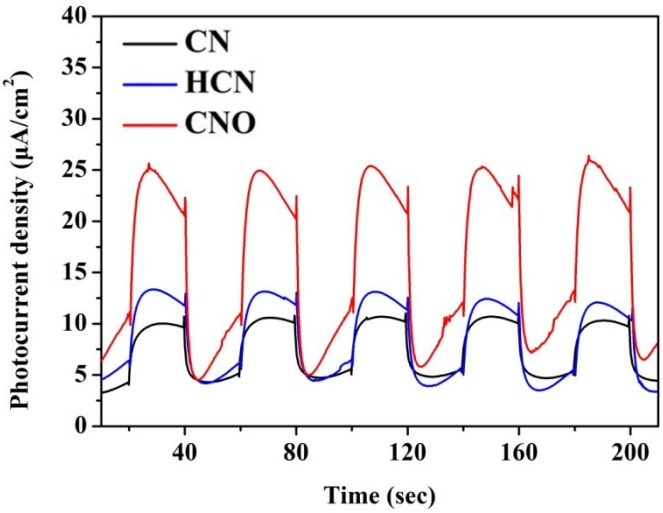

Fig. S10 Transient photocurrent responses of CN, HCN and CNO samples.

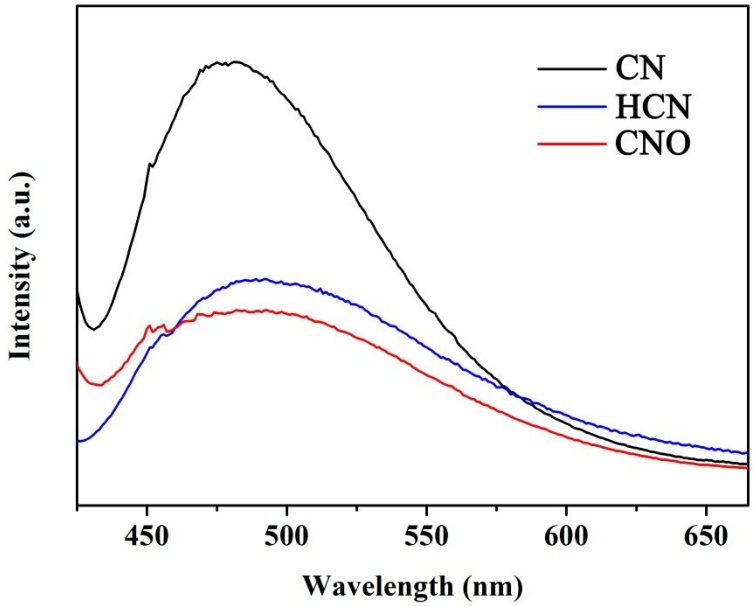

Fig. S11 PL spectra of the CN, HCN and CNO sample.

Table S1. OEA of the CNO-precursor and commercial MA.

Sample	N%	C%	H%	O%
Precursor of CNO	**55.90**	**23.90**	**6.276**	**0.353**
Commercial MA	**28.36**	**66.66**	**4.92**	**None**

Table S2. OEA of the CNO, HCN and CN sample.

Sample	N%	C%	H%	O%
CNO	**61.59**	**32.33**	**1.417**	**4.592**
HCN	**63.65**	**34.26**	**1.680**	**0.289**
CN	**63.47**	**34.68**	**1.474**	**0.348**

AQE Calculation

The detailed calculating method of AQE is as follows.

The testing points for irradiation intensity were selected at solution surface. Based on commercial testing guideline, there are four edge points and one center point, as shown as follows.

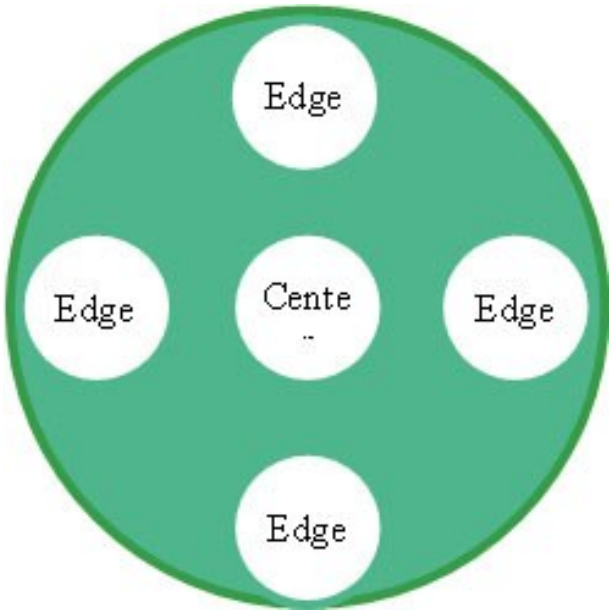

Average irradiation intensity: (W·m^{-2})

$$\bar{E} = \frac{1}{3}E_{Center} + \frac{2}{3}E_{Edge}$$

Irradiation area: (m^{-2})

$$A_R = \pi R^2$$

Average irradiation fluxes: (W)

$$P = \bar{E} \cdot A_R$$

Number of incident photons:

$$N_P^i = \frac{Pt\lambda}{hc}$$

Number of electron transferred:

$$N_e = 2 \cdot n_{H_2} \cdot N_A$$

Apparent quantum yield:

$$AQE\% = \frac{N_e}{N_P^i} \times 100\%$$

Taking λ=420±10 nm as an example, the calculating results are presented in the following **Table S3**.

	E_{edge} (W·m^{-2})				E_{center} (W·m^{-2})			$\bar{E}$(W·m^{-2})
	1	2	3	4				
Test values	5.0 5.2 5.3	3.2 3.8 4.0	3.5 3.6 3.7	6.8 6.9 7.1	12.3	12.5	12.1	7.3
Average values	4.8				12.3			

$A_R = \pi R^2 = 3.1416 \times 0.025^2 = 0.00196\ m^2$ (irradiation area)

$$N_P^i = \frac{Pt\lambda}{hc} = \frac{7.3 \times 0.00196 \times 3600 \times 420 \times 10^{-9}}{6.626 \times 10^{-34} \times 2.997 \times 10^8} = 1.089 \times 10^{20}$$

$$N_e = 2 \cdot n_{H_2} \cdot N_A = 2 \times 1.180 \times 10^{-5} \times 6.022 \times 10^{23} = 1.421 \times 10^{19}$$

$$AQE\% = \frac{N_e}{N_P^i} \times 100\% = \frac{1.421 \times 10^{19}}{1.089 \times 10^{20}} \times 100\% = 13.04\%$$

Table S4 Comparison of the photocatalytic performance in hydrogen evolution of CNO with other recently reported carbon nitrides.

Catalyst	**Lamp**	**HER (μmol·h^{-1}·g^{-1})**	**BET surface area (m^2·g^{-1})**	**Normalized HER (μmol·h^{-1}·m^{-2})**	**AQE (%)**	**Reference**
Holey O-doped g-C_3N_4 thin sheet	λ>420 nm	6752	348.0	19.4	-	1
O-doped g-C_3N_4	λ>420 nm	375	47.0	7.98	-	2
O-doped porousg-C_3N_4	λ>420 nm	1204	36.1	33.3	7.8	3
Porous ultrathin O-doped g-C_3N_4 nanosheets	λ>400 nm	3786	109.3	34.6	-	4
Porous O-doped g-C_3N_4 nanosheets	λ>400 nm	1748.6	48.9	35.7	7.2	5
Mesoporous S-doped g-C_3N_4	λ>420 nm	1360	128.4	10.6	5.8	6

C-rich g-C_3N_4 nanosheet	λ>400 nm	3960	213.2	18.6	4.52	7
C-incorporated g-C_3N_4	λ>400 nm	793	34.9	22.7	-	8
N-deficient g-C_3N_4	λ>420 nm	316	10.4	30.4	-	9
O-doped g-C_3N_4 nanosheet without porous structures	λ>420 nm	1050.3	31.7	33.1	13.04	**This work**

Reference

1 S. Guo, Y. Zhu, Y. Yan, Y. Min, J. Fan and Q. Xu, *Appl. Catal. B-Environ.*, 2016, **185**, 315.

2 J. Li, B. Shen, Z. Hong, B. Lin, B. Gao and Y. Chen, *Chem. Commun.*, 2012, **48**, 12017.

3 Z. F. Huang, J. J. Song, L. Pan, Z. M. Wang, X. Q. Zhang, J. J. Zou, W. B. Mi, X. W. Zhang and L. Wang, *Nano Energy*, 2015, **12**, 646.

4 X. She, L. Liu, H. Ji, Z. Mo, Y. Li, L. Huang, D. Du, H. Xu and H. Li, *Appl. Catal. B-Environ.*, 2016, **187**, 144.

5 C. Wang, H. Q. Fan, X. H. Ren, J. W. Ma, J. W. Fang and W. J. Wang, *ChemSusChem*, 2018, 11, 700.

6 J. Hong, X. Xia, Y. Wang and R. Xu, *J. Mater. Chem.*, 2012, **22**, 15006.

7 Y. F. Li, M. Yang, Y. Xing, X. C. Liu, Y. Yang, X. Wang and S. Y. Song, *Small*, 2017, **13**, 8.

8 W. N. Xing, C. M. Li, G. Chen, Z. H. Han, Y. S. Zhou, Y. D. Hu and Q. Q. Meng, *Appl. Catal. B-Environ.*, 2017, **203**, 65.

9 Z. Hong, B. Shen, Y. Chen, B. Lin and B. Gao, *J. Mater. Chem. A*, 2013, **1**, 11754.